American Mineralogist, Volume 67, pages 587–598, 1982

The crystal structure of lizardite 1*T*: hydrogen bonds and polytypism

MARCELLO MELLINI

C.N.R., C.S. Geologia Strutturale e Dinamica dell'Appennino
Via S. Maria 53, 56100 Pisa, Italy

Abstract

The occurence of lizardite 1*T* from Val Sissone, Italy, is reported. Electron microprobe analysis leads to the doubled unit cell content

$$(Mg_{5.58}Fe^{2+}_{0.08}Fe^{3+}_{0.20}Al_{0.14})\ (Si_{3.66}Al_{0.34})O_{10.00}(OH)_{8.00}.$$

The unit cell parameters are a = 5.332(3)Å, c = 7.233(4)Å, space group is $P31m$.

The crystal structure has been refined, using 209 symmetry independent reflections, to R = 0.031. The refined model is not far from the idealized geometry of the serpentine layer. The ditrigonal distortion of the six-membered tetrahedral ring is small ($\alpha = -3.5°$). No buckling of the brucite-like sheet is observed.

The occurrence of both negative and positive α values in serpentine minerals is explained on the basis of stacking sequence and hydrogen bonds. Namely, the best hydrogen bond system is attained by rotation of the bridging oxygens belonging to the tetrahedral sheet. The direction of rotation depends on the way in which subsequent layers are stacked one upon the other. The substitution of trivalent atoms for magnesium and silicon leads to stronger hydrogen bonding between adjacent layers, thus promoting the formation of flat-layer structures and increasing thermal stability.

Introduction

The well-known classification of the serpentine minerals was developed by Whittaker and Zussmann (1956). The scheme is based on the recognition of cylindrical layers in chrysotile, corrugated layers in antigorite, and flat layers in lizardite. A recent review of the crystal structure of the serpentine minerals was given by Wicks and Whittaker (1975). The most serious handicap to full understanding of the serpentine structures is the low degree of three-dimensional order present in these minerals. For instance, the previous two-dimensional determinations of the crystal structure of lizardite, by Rucklidge and Zussman (1965) and by Krstanovic (1968), led to discrepancy factors of 18 percent and 19 percent respectively, in spite of the fact the flat-layer lizardite structure would seem to be the most promising for X-ray diffraction analysis.

Lizardite from Kennack Cove (Rucklidge and Zussman, 1965) is composed of domains of 1*T* and disordered 2*H* polytypes. Lizardite from Radusa Mine (Krstanovic, 1968) is composed of the 1*T* polytype. According to Rucklidge and Zussman (1965), the average crystal structure has trigonal symmetry, but Krstanovic (1968) refined his model in the space group *Cm*. Subsequently, Wicks and Whittaker (1975), in discussing Krstanovic's refinement, stated that lizardite 1*T* "is in fact orthorhombic and only pseudo-trigonal".

Wicks and Whittaker (1975) and Krstanovic (1980) have discussed the distortions of both the tetrahedral and the octahedral sheets of a very pure lizardite 1*T* with limited substitutions for silicon or magnesium. According to these authors, the composition of lizardite 1*T* from Radusa Mine results in a large misfit between the tetrahedral and octahedral sheets, and produces shifts of the atoms away from the ideal positions. In particular, they noted buckling of the plane of the magnesium atoms and various shifts, along [001], of the oxygen, silicon and magnesium atoms. In this present paper, I report a more regular model for the crystal structure of lizardite 1*T* from Val Sissone, Italy, that contains significant aluminum and iron substitution. The structure is not very different from the idealized geometry of the serpentine layer and was refined using diffraction data obtained on euhedral crystals of lizardite 1*T*. The different composition of the Val Sissone lizardite 1*T*, with its different structural constraints, limits comparison with the lizardite 1*T*

0003–004X/82/0506–0587$02.00

structure of Krstanovic (1968), but does provide important structural details of a composition intermediate between the slightly substituted lizardite 1*T* of Krstanovic and more aluminous structures such as the 9*T* polytype of Jahanbagloo and Zoltai (1968).

Occurrence

Few data about the occurrence of lizardite 1*T* in Val Sissone, Italy, are available. All the observed material occurs in a small rock fragment nearly 1 cm^3 in volume. The fragment is composed mainly of saccharoidal dolomite with abundant yellow orange clinohumite. A vein of lizardite crystals, up to 1 mm thick, cuts through the rock fragment. According to the collector, Dr. Edgar Huen, the fragment was detached some years ago from an erratic block in the Val Sissone moraine. Subsequent attempts to locate the block have been unsuccessful. Val Sissone is in the contact zone, composed of carbonate, calc-silicate rocks and amphibolites, that is associated with the Bergell granite (Wenk and Maurizio, 1970; Trommsdorf and Evans, 1972 and 1977). Calcite, dolomite, diopside, amphiboles, spinel and chondrodite occur in this zone.

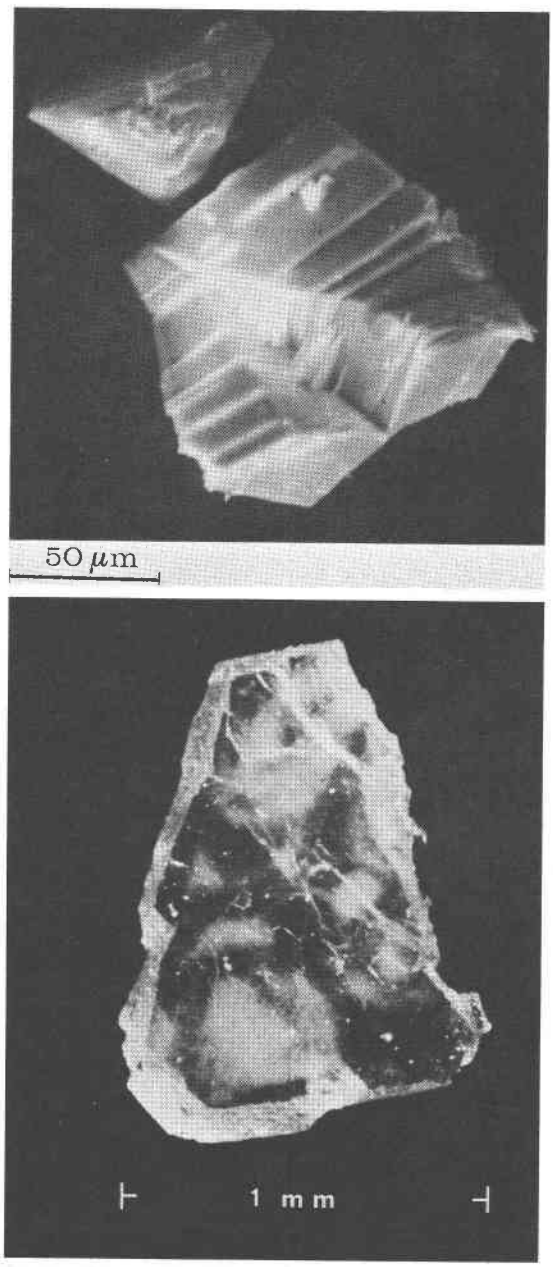

Fig. 1. a) Crystals of lizardite 1*T*, observed by SEM; b) Photograph of a large crystal of lizardite 1*T*.

The crystals are light yellow in color, and their crystal habit ranges from trigonal plates to truncated trigonal pyramids, depending on the crystal thickness. A similar habit has been observed for the related mineral cronstedtite $(Fe_2^{2+}Fe^{3+})(SiFe^{3+})O_5(OH)_4$ (Steadman and Nuttall, 1963). The lizardite crystals are equant and reach 0.2 mm in diameter. Examination by SEM shows the presence of euhedral crystals as well as less regular aggregates. One of these aggregates is shown in Figure 1a, together with a more regular, rather thin, truncated triangular pyramidal crystal. The morphology is consistent with the point group *3m*. The micrograph shows that the aggregates consist of several individual (001) plates, stacked one upon the other. Sometimes, adjacent plates are slightly rotated around [001]. Finally, the rims of the thin outer plates appear not absolutely flat, but partially bent. Larger crystals of lizardite 1*T* have also been found. Figure 1b is a light optical photograph of a large crystal of lizardite 1*T*, whose astonishing, larger dimension reaches 2 mm. It is a detached crystal, found by Dr. Edgar Huen in the same environment where the rock fragment was collected, and has the same properties as the vein crystals.

Chemical analysis

The preliminary qualitative chemical investigation, by energy dispersive analysis during the SEM observation, revealed abundant silicon and magnesium with lower contents of iron and aluminum. The quantitative chemical data were gathered by an ARL-SEMQ electron microprobe, equipped with crystal spectrometers, using 15 kV accelerating voltage, 20 nA specimen current, an approximate 5 μm diameter electron beam and standard Bence Albee correction procedures. The estimated standard deviations on oxide contents, obtained from

Table 1. Electron microprobe analysis of lizardite 1*T* from Val Sissone, Italy

	weight percent	atoms per cell
SiO_2	39.8	1.83
MgO	40.9	2.79
Al_2O_3	4.5	0.24
Fe_2O_3 *	2.9	0.10
FeO *	1.0	0.04
F	not detected	-
	89.1	
H_2O **	10.9	1.67

* Total iron was shared between the two oxidation states to assure full occupancy of the cationic sites and charge balance.

** Calculated by difference

counting statistics, range from 0.3 to 2.5 relative percent, depending on the abundance of the element. As four analyses on two different grains did not show variations in oxide contents larger than 1 relative percent for more abundant elements and larger than 5 relative percent for less abundant elements, the analyses were averaged to produce the data reported in Table 1.

The ferrous and ferric contents were calculated from the determined iron value by assuming full occupancy of the cationic sites by silicon, magnesium, iron and aluminum (five cations per unit cell) and charge balance. This statement is based on the assumption that, for each silicon atom which is substituted by a trivalent cation, one trivalent cation must be substituted for the divalent magnesium in octahedral coordination. The water content, calculated by difference from 100 weight percent, of 10.9 wt.% is lower than the expected of 13 wt.%. The water deficiency may be due to unknown analytical errors, as well as to dehydration of lizardite under the electron beam, with a subsequent biased, slightly high determination of the other oxides. Unfortunately, the shortage of material prevented an independent determination of the water content.

The analytical data lead to a formula calculated on the basis of charge balance and five cations per unit cell of

$$(Mg_{2.79}Fe^{2+}_{0.04}Fe^{3+}_{0.10}Al_{0.07})(Si_{1.83}Al_{0.17})O_{5.33}(OH)_{3.34},$$

where all the iron atoms are assumed as octahedrally coordinated. The addition of 0.33 water molecules to compensate for the water assumed lost during analysis produced the slightly idealized formula

$$(Mg_{2.79}Fe^{2+}{}_{0.04}Fe^{3+}{}_{0.10}Al_{0.07})(Si_{1.83}Al_{0.17})O_{5.00}(OH)_{4.00}.$$

The calculated densities are 2.575 and 2.630 g cm^{-3} for the actual and the idealized formula, respectively, while the experimental value, determined by the heavy liquid method, is 2.58(1) g cm^{-3}.

Comparison with the chemical data discussed by Whittaker and Wicks (1970) shows that the most interesting feature of the Val Sissone lizardite is probably the high Al_2O_3 content (4.5 wt.%). Similar values have been obtained by hydrothermal synthesis of one layer and similar, as well as higher values, have been reported for synthesized multi-layer lizardite (Caruso and Chernosky, 1979). They are known also for naturally occurring multi-layer lizardite (Jahanbagloo and Zoltai, 1968 and Wicks and Plant, 1979) and single-layer lizardite (Frost, 1975; Dungan, 1979).

X-ray crystallography

Lizardite 1*T* from Val Sissone produces very sharp diffraction spots. Streaking or diffuseness, indicating partial disorder, are rarely observed. Weissenberg and precision photographs, as well as intensity data collected by single crystal counter methods lead to an unambiguous determination of the Laue symmetry $\bar{3}m$. No systematic extinctions were observed, thus leading to the possible choice between $P31m$ and $P\bar{3}1m$ space groups, with cell parameters $a \simeq 5.3$Å, $c \simeq 7.2$Å. The centrosymmetric space group was ruled out, based on the noncentrosymmetric arrangement of atoms in the serpentine structure and on the point group suggested by morphological observation. Overexposed rotation photographs do not show any c periodicity larger than 7.2Å.

A tiny euhedral crystal of lizardite (nearly 0.1 × 0.1 × 0.15 mm^3), with a trigonal truncated pyramidal habit, was chosen for the refinement of the unit cell parameters and for collection of the intensity data, on a Philips PW 1100 single crystal automated diffractometer, equipped with graphite-monochromatized molybdenum Kα radiation. The unit cell parameters, refined by least squares fitting of the crystal setting for 25 reflections, converged to the

Table 2. X-ray powder diffraction pattern of lizardite 1*T* from Val Sissone, Italy

$d_{obs.}$	$d_{calc.}$	hkl	I
7.216	7.238	001	s
4.628	4.623	100	m
3.890	3.896	101	m
3.624	3.619	002	ms
2.850	2.850	102	w
2.668	2.669	110	vw
2.506	2.504	111	s
2.418	2.413	003	vw
2.152	2.148	112	ms
1.948	1.948	202	vw
1.790	1.790	113	ms
1.748	1.747	210	vw
1.701	1.699	211	vw
1.676	1.669	203	vw
1.575	1.574	212	vw
1.539	1.541	300	m
1.506	1.507	301	w
1.498	1.498	114	w
1.418	1.418	302	vw
1.335	1.335	220	vw
1.314	1.312	221	w

values $a = 5.332(3)$Å, $c = 7.233(4)$Å. These values are not significantly different from those obtained by least squares fitting of the X-ray powder diffraction pattern, $a = 5.338(2)$Å and $c = 7.238(3)$Å. The pattern (Table 2) was obtained with a Gandolfi camera (57.3 mm in diameter) and cobalt Kα radiation on a single crystal, previously identified by rotation and Weissenberg photographs.

A total of 338 reflections, belonging to two equivalent sets in the Laue group $\bar{3}m$, was measured from 3 to 25°Θ using a Θ–2Θ scan and a scan width of 1.40°. Intensity data for 121 reflections were not collected during this step, as a pre-scan showed $I_{peak} - 2\sqrt{I_{peak}} < I_{back}$, with I_{peak} and I_{back} indicating peak intensity and background intensity, respectively. No crystal decay or instrumental drift was observed. The data were corrected for Lorentz and polarization factors. No absorption correction was made, owing to the small dimensions of the crystal and the low absorption coefficient. Symmetrically-equivalent reflections were averaged to produce an unique set of 209 reflections; the discrepancy factor $R_{eq} = [\Sigma_{all}\ (n\Sigma_i w_i\ (\bar{F}-F_i)^2)/\Sigma_{all}((n-1)\Sigma_i w_i F_i^2)]^{1/2}$, calculated among the n symmetry related reflections, was 0.04.

The trial model, derived from the idealized structure in the space group $P31m$, was easily refined with isotropic temperature factors to $R = \Sigma||F|_o - |F_c||/\Sigma|F_o| = 0.047$. The introduction of two independent hydrogen atoms, located by a F_o map, lowered the R to 0.042. Further refinement, using isotropic temperature factors for the heavy atoms and anisotropic temperature factors for the hydrogen atoms lowered the R to 0.031. No peak higher than 0.3 eÅ^{-3} was observed in the final ΔF synthesis. Scattering factors for neutral atoms were taken from the *International Tables for X-Ray Crystallography, vol. IV* (1974). Final atomic thermal and positional parameters are reported in Table 3. Observed and calculated structure factors are given in Table 4[1].

[1] To receive a copy of Table 4, order Document AM-82-201 from the Business Office, Mineralogical Society of America, 2000 Florida Avenue, N.W., Washington, D.C. 20009. Please remit $1.00 in advance for the microfiche.

Table 3. Final atomic positional and thermal parameters. Esd's are in parentheses

	x	y	z	U_{11}	U_{22}	U_{33}	U_{23}	U_{13}	U_{12}
Si	1/3	2/3	0.0766(7)	50(4)	50(4)	116(8)	25(2)	0	0
Mg	0.3327(5)	0	0.4596(7)	32(4)	32(4)	122(7)	16(2)	7(9)	0
O1	1/3	2/3	0.3000	96(12)	96(12)	68(21)	48(6)	0	0
O2	0.5087(11)	0	-0.0036(9)	130(12)	130(12)	136(17)	65(6)	48(20)	0
O3	0.6654(10)	0	0.5935(7)	95(9)	95(9)	91(15)	48(5)	-3(20)	0
O4	0	0	0.3088(14)	58(17)	58(17)	161(34)	29(8)	0	0
				U					
H3	0.655(5)	0	0.709(5)	0.026(5)					
H4	0	0	0.199(5)	0.001(5)					

Anisotropic temperature factors ($\times 10^4$) are of the form:
$\exp[-2\pi^2(U_{11}h^2a^{*2} + U_{22}k^2b^{*2} + U_{33}l^2c^{*2} + 2U_{12}hka^*b^* + 2U_{13}hla^*c^* + 2U_{23}klb^*c^*)]$.

Structure description

The main features of the crystal structures of the serpentine minerals are well established (Wicks and Whittaker, 1975). As shown in Figures 2 and 3, 1:1 layers, consisting of a silicate tetrahedral sheet and a brucite-like magnesium octahedral sheet, alternate along [001]. The linkage between adjacent layers is strengthened by hydrogen bonds. Although the general arrangement is known, the presence of stacking disorder in most lizardites has prevented the determination of the three dimensional arrangement of atoms within the layer. Because of the absence of random stacking shifts the lizardite 1*T* from Val Sissone appears to be truly trigonal, at least within the limits of the present refinement (R = 0.031). No indication of orthorhombic (Wicks and Whittaker, 1975) or monoclinic symmetry (Krstanovic, 1980) was recorded. In spite of the trigonal symmetry, the Val Sissone lizardite 1*T* can be alternately described by a *C*-centered metrically orthorhombic unit cell, for easier comparison with the data available for lizardite and the other serpentine minerals. Its parameters are a = 5.332Å, b = 9.235Å, c = 7.233Å. The unit cell content may be doubled to

$$(Mg_{5.58}Fe^{2+}_{0.08}Fe^{3+}_{0.20}Al_{0.14})$$

$$(Si_{3.66}Al_{0.34})O_{10.00}(OH)_{8.00},$$

for comparison with the popular formula $(Mg_{6-x}Al_x)\ (Si_{4-x}Al_x)O_{10}(OH)_8$.

The deviations from idealized geometry for the Val Sissone lizardite structure are rather small. For instance, the ditrigonal tetrahedral sheet is characterized by remarkable hexagonal pseudosymmetry (Fig. 2) because the rotation of tetrahedra towards the ditrigonal configuration is quite small (α = −3.5°).

The presence of several symmetry constraints, due to the trigonal symmetry, leads to the existence of a few (x,y) planes where the atoms are located. It is therefore possible to locate both the basal oxygen plane and the silicon plane of the tetrahedral sheet and both the magnesium plane and an outer oxygen plane of the octahedral sheet. Moreover, the oxygen atoms common to both the tetrahedral and octahedral sheet do not deviate too much from the geometrical plane. Indeed, the z heights of O1 and O4 atoms differs only by 0.064Å instead of 0.3Å, as reported by Krstanovic for the magnesium rich lizardite 1*T*. Also, no buckling of the plane of

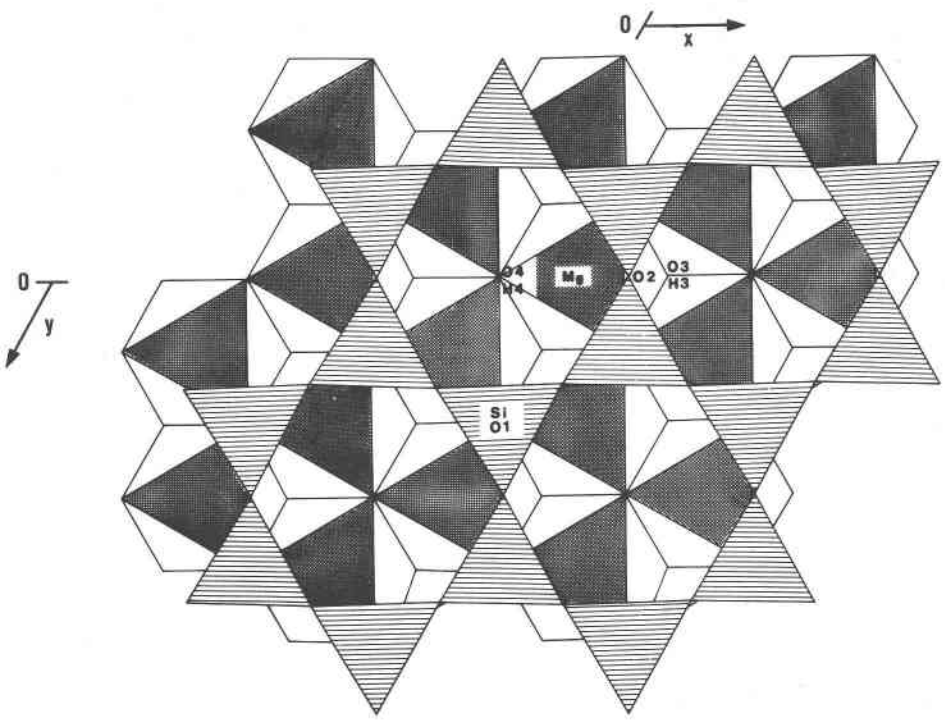

Fig. 2. 1 : 1 layer of lizardite 1*T*, viewed along [001].

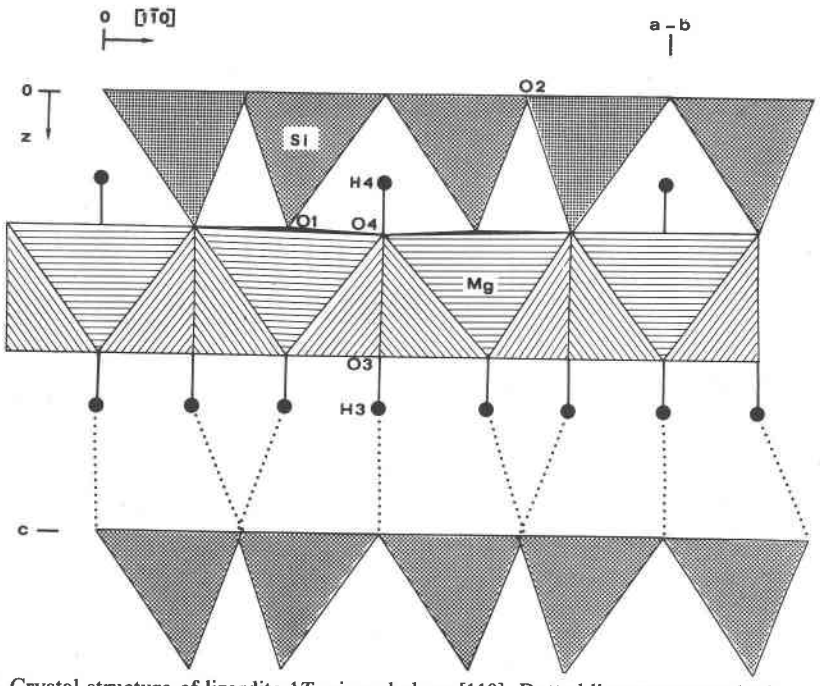

Fig. 3. Crystal structure of lizardite 1*T*, viewed along [110]. Dotted lines represent hydrogen bonds.

magnesium atoms was found in the Val Sissone lizardite 1*T*.

Silicon coordination

Only one independent silicon atom is present per unit cell. It forms three long bonds (1.646Å) with the bridging O2 oxygen atoms and one short bond (1.616Å) with the non bridging O1 oxygen atom (Table 5). The average Si–O bond distance, 1.639Å, is larger than expected for unsubstituted silicon tetrahedra (Baur, 1978) but is in agreement with the chemical data, which suggest substitution of silicon by aluminum. The possible substitution by iron seems unlikely and, in fact, Rozenson *et al.* (1979) did not find trivalent iron in tetrahedral coordination during the Mössbauer analysis of several lizardites. Moreover, assuming a linear relationship between the average tetrahedral bond distance and the aluminum content and taking into account the different coordinations of the oxygens, the ionic radii reported by Shannon and Prewitt (1969) indicate an aluminum site population of 0.11. Therefore, it seems justified to assume that the tetrahedral site is occupied by nearly 0.9 silicon atoms and 0.1 aluminum atoms.

Finally, the Si–O–Si configuration is rather regular and the non-bonded Si–Si distances, the Si–O–Si angles and the related Si–O bond distances are in aggreement with the results of the statistical analysis of Si–O–Si configurations by O'Keefe and Hyde (1978).

Magnesium coordination

The coordination polyhedron around Mg is a trigonal antiprism (flattened octahedron). It is represented in Figure 4 by the corresponding Schlegel diagram. The diagram is obtained by contraction of the upper face of the polyhedron and enlargement of the lower face, so as to show all the polyhedral edges. The thickness of the octahedral sheet along [001] ranges from 2.06Å (measured between O1 and O3 atoms). The value is lower then the 2.20Å previously reported for lizardite 1*T* and is closer to the thickness found in other serpentine minerals (Wicks and Whittaker, 1975) and brucite (2.11Å). The bond distances range from 2.021Å to 2.082Å for the Mg-OH bonds and are 2.121Å long for both the Mg–O bonds formed with the silicon bonded O1 oxygens (Table 5). Inspection of the bond distances and O–O distances shows that the octahedral atom is shifted from the center of the octahedron towards the outer O3 plane. This feature can be related to the donor behavior of O3 atoms in the hydrogen bonds that develop between adjacent layers.

The average bond distance, 2.067Å, is smaller than the value of 2.10Å computed from the ionic

radii given by Shannon and Prewitt (1969). The smaller dimensions of the coordination polyhedron are in keeping with the chemical data, which suggest substitution by aluminum and trivalent iron for magnesium.

Hydrogen bond system

Two crystallographically-independent hydrogen atoms are present in the crystal structure. Both hydrogen atoms were located in the F_o map and their positions were refined. One of them, H4, which is located in the center of the ditrigonal ring, does not form any hydrogen bond. The other one, H3, links adjacent layers through hydrogen bonds formed between the donor O3 and the acceptor O2 oxygen atoms. The hydrogen bond is weak, 0.094 v.u. according to Lippincott and Schroder (1955), due to the long O2–O3 distance (3.03Å). However, the relative weakness of the single hydrogen bond is balanced by the high number of bonds (one hydrogen bond per 8.2Å^2).

Bond strength balance

The bond strength calculations (Table 6) were made according to Brown and Wu (1976), using the same parameters $R_1 = 1.622$ and $N = 4.290$ for both tetrahedral and octahedral cations. Taking into account the hydrogen bond contribution, the sums of bond strengths reaching the anions closely fit the theoretical values and the discrepancies are always lower than 0.07 v.u. On the other hand, the sums of bond strengths reaching the cations are significantly higher than two and lower than four, for the octahedral and tetrahedral site, respectively, further supporting the substitution of trivalent atoms in the two sites.

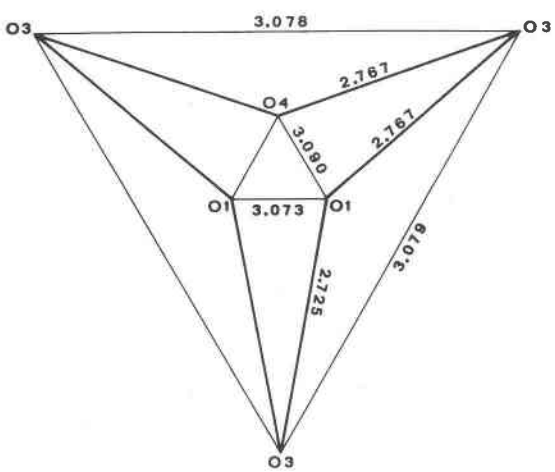

Fig. 4. The octahedral site, represented by Schlegel diagram. Heavy lines represent shared edges.

Table 5. Bond lengths (Å) and bond angles (°) in lizardite 1*T* Esd's are in parentheses.

Si1-O1	1.616(5)	Mg-O3	2.021(5)
-O2	1.646(3) x3	-O3	2.026(5) x2
average	1.639	-O4	2.082(5)
		-O1	2.121(3) x2
		average	2.067
O2-O2	2.667(5)		
O2-O1	2.682(5)	Si-Si	3.078(3)
O2-Si1-O2	108.3(3)	Si-O2-Si	138.6(3)
O1-Si1-O2	110.6(3)		
O3-H3	0.84(6)	O4-H4	0.79(6)

All the results of the refinement, particularly the bond distances and bond strength balance, support the crystal chemical formula

$$(Mg_{5.58}Fe^{2+}_{0.08}Fe^{3+}_{0.20}Al_{0.14})(Si_{3.66}Al_{0.34})O_{10.00}(OH)_{8.00},$$

previously proposed on the basis of the chemical data.

Polytypism and hydrogen bonding

Ditrigonal distortion and hydrogen bonding

As previously stated, the six-membered tetrahedral ring is distorted toward the ditrigonal configuration, due to alternate rotation of the bridging oxygen atoms. In the present case the oxygen atoms move away from the nearest magnesium atoms within the same layer and toward the hydroxyl groups of the adjacent layer. The rotation can be described by the value $\alpha = -3.5°$, where the minus sign means movement away from the atoms in octahedral coordination. In the nomenclature proposed by Franzini (1969) for the mica layer, negative rotations correspond to *B* layers and positive rotations correspond to *A* layers. *B* layers occur infrequently in layer silicates and, in the serpentine minerals, they have been previously reported for only the 9-layer serpentine (Jahanbagloo and Zoltai, 1968; $\alpha = -8°$). *A* layers occur in two amesites $2H_2$, from Saranovskaie (Steinfink and Brunton, 1962; Anderson and Bailey, 1981; $\alpha = +14.7°$) and from Antarctic (Hall, 1974; Hall and Bailey, 1979; $\alpha = +13.6°$ and $+14.5°$). There are also other structures of serpentine minerals where *A* layers have been

Table 6. Bond strength balance (v.u.), calculated according to Brown and Wu (1976) and Lippincott and Schroder (1955).

	Mg	Si	Σc_v	Hydrogen bond contribution	$\Sigma c'_v$
O1	0.316x3 0.316	1.016	1.964		1.964
O2		0.939x2	1.878	+0.094	1.972
O3	0.389 0.386 0.386		1.161	-0.094	1.067
O4	0.343x3		1.029		1.029
Σa_v	2.136	3.833			

Σc_v = sums of bond strengths to the anion.
$\Sigma c'_v$ = sums of bond strengths to the anion, after correction for the hydrogen bond.
Σa_v = sums of bond strengths to the cation.

reported. These are the Unst-type serpentine (lizardite $6T_1$) and its Mg–Ge synthetic analogue (Hall *et al.*, 1976), amesite $6R_2$ (Steadman and Nuttall, 1962) and the $1T$, $6R_2$, $3T_1$ polytypes of cronstedtite (Steadman and Nuttall, 1963). Unfortunately, these last six structure analyses are less accurate because of poor experimental data. Their R factors range from 0.15 to 0.21, the refinements do not take into account cation ordering (Bailey, 1975) and, in some cases, the A configuration has been assumed by analogy with other structures. As a consequence, the details of these refinements are less reliable.

In the four structures for which three-dimensional refinements are available, the bridging oxygen atoms always move toward the hydroxyl groups belonging to the adjacent layer. Therefore, either A or B layers are present, and stronger hydrogen bonding is achieved in these serpentine structures. Similar movement towards the hydroxyl groups occurs also in the Unst-type serpentine and its Mg–Ge synthetic analogue (Hall *et al.*, 1976), amesite $6R_2$ (Steadman and Nuttall, 1962), cronstedtite $3T_1$ (Steadman and Nuttall, 1963). The opposite movement, away from the hydroxyl groups, has been reported for cronstedtite $1T$ and $6R_2$ (Steadman and Nuttall, 1963). Unfortunately, the details of these six last structure analyses cannot be confidently used in this discussion. It is conceivable that, as shown by the best four available studies, the presence of A or B layers in the serpentine minerals depends on which configuration leads to more efficient interlayer hydrogen bonding. The importance of interlayer hydrogen bonding with regard to the ditrigonal distortion of the tetrahedral sheet also is supported by the available data on layer silicates other than serpentine minerals. In fact, in chlorite the movement of the bridging oxygen atoms always leads to stronger hydrogen bonds, by B layers in the case of Ib-chlorite and by A layers in the case of Ia and IIb-chlorite (Shirozu and Bailey, 1965). On the other hand, only A layers occur in mica (Baronnet, 1976) or in talc (Rayner and Brown, 1973), where no hydrogen bond can form.

Experimental and theoretical results

Peterson *et al.* (1979) performed molecular orbital calculations on the clusters $[Mg_3F_6(OH)_7Si_6O_6F_6]^{1-}$ and $[Mg_4F_{12}(OH)_3Si_3O_3F_5]^{6-}$. The clusters were used to model the serpentine 1 : 1 layer. By definition, the model does not take into account interlayer effects. Assuming 1.62Å as the value of the Si–O bond distance, minima in the total energy curve are found at $\alpha = -2.1°$ and $\alpha = -3.9°$, for the trimeric and the tetrameric unit, respectively. The results fit the experimental data for the Val Sissone lizardite $1T$, which has an average Si–O distance of 1.639Å and $\alpha = -3.5°$.

When the calculation is performed for a tetrahedral sheet with greater substitution, using 1.68Å as the average tetrahedral bond distance, two minima are found. The lower minimum is at $\alpha = -12.3°$ and the higher energy minimum is at $\alpha = +12.7°$ for the trimeric unit and at $\alpha = -13.8°$ and $\alpha = +10.6°$ for the tetrameric unit. Assuming that the energy curves and their minima are not model dependent

but physically sound, some important remarks can be made:

(1) *B* layers are expected for tetrahedral sheets with lower substitution for silicon. This theoretical result fits the experimental data for the Val Sissone lizardite 1*T*, which has $\alpha = -3.5°$.

(2) *B* layers are expected also for tetrahedral sheets with greater substitution for silicon. Actually, they occur in the 9-layer serpentine (Jahanbagloo and Zoltai, 1968), which has an average Si–O bond distance of 1.66Å and $\alpha = -8°$. However, the existence of a higher energy minimum suggests the possible existence of *A* layers for aluminum-rich disordered flat-layer serpentines. The choice of the positive, or negative, rotation might then be determined by interlayer effects, namely by the stabilization energy associated with the formation of hydrogen bonds. Although *A* layers occur in amesite $2H_2$ (Hall and Bailey, 1979; Anderson and Bailey, 1981), no close comparison can be made, as the disordered CNDO/2 model by Peterson *et al.* (1979) is not strictly applicable to the ordered layer of amesite $2H_2$.

(3) Assuming that *A* and *B* layers may exist independently in aluminum-rich flat-layer serpentines, the simultaneous occurrence of both *A* and *B* layers within the same complex polytype may be expected.

Polytypic sequence and ditrigonal distortion

A close relationship between the *A* or *B* nature of the layer in the serpentine minerals and the stacking operator can be found. Disregarding possible interlayer shifts, Figure 2 clearly shows that shorter OH–O distances will result in *B* layers and longer OH–O distances will result in *A* layers if the stacking sequence does not include ± 60° or 180° rotation (*r* rotation according to Bailey, 1969, and Wicks and Whittaker, 1975). Otherwise, the presence of the *r* rotation leads to shorter OH–O distances by *A* layers and to longer OH–O distances by *B* layers. Therefore, *B* layers must be expected when the stacking sequence does not include *r* and *A* layers when the stacking operator includes *r*. If the possible interlayer shifts ($a/3$, $\pm b/3$, as they were defined by Bailey, 1969, and Wicks and Whittaker, 1975) are also taken into account, similar relationships are derived. The complete results are given in Table 7.

The layer configurations reported in Table 7 were obtained assuming that the formation of hydrogen bonds controls the direction of the movement of the bridging oxygen atoms in flat-layer serpentines, which is indicated by the few, reliable data on these minerals. The Table 7 can be eventually used to predict the direction of movement of the bridging oxygens in other polytypes, whose structure is not known. More complex polytypes, not included in Table 7, can be analyzed by examination of the stacking sequence and reduction of the long, complex sequence to the sum of shorter sequences, as in the case of the 9-layer serpentine (Jahanbagloo and Zoltai, 1968).

Misfit relief and interlayer bonding

The aluminum content is a very important parameter in the crystal chemistry of the serpentine

Table 7. Relationship between the stacking sequence operator and ditrigonal distortion of the tetrahedral sheet.

Interlayer shift	Layer configuration	Polytypes *	Examples
None	B	1T	Lizardite 1T from Val Sissone
r	A	$2H_1$	Not known
a/3	A	1M, $2M_1$, $3T_1$	Not known
r+a/3	B	2Or, $2M_2$, $6H_1$	Not known
b/3	B	3R, 2T, $6R_2$, $3T_2$	Not known
r+b/3	A	$2H_2$, $6R_1$	Amesite $2H_2$ (Saranovskaie and Antarctic)
r b/3+r	A	$6R_3$, $6H_2$	Not known

* More complex polytypes can be analyzed by examination of the stacking sequence (for example, in the 9-layer serpentine (Jahanbagloo and Zoltai, 1968) the sequence is "none, a/3+r, -a/3+r", repeated three times.

minerals. Although no sharp compositional break between flat-layer and curved-layer serpentines or between single-layer and multi-layer lizardites has been observed (Jasmund and Sylla, 1971 and 1972; Wicks and Whittaker, 1975; Wicks and Plant, 1979), the greater substitution of aluminum for silicon and magnesium leads to more stable structures (Caruso and Chernosky, 1979) and promotes flat-layer lizardites (Wicks and Whittaker, 1975). The aim of this section is to explain how aluminum stabilizes the structure. It is not my purpose to assert here that aluminum is an essential component of flat-layer structures, or that it must be absent in curved-layer serpentines.

It is generally accepted that the usual disorder in serpentine minerals is due in part to the mismatch in dimensions of the larger octahedral and smaller tetrahedral sheets (*e.g.*, Radoslovich, 1962; Wicks and Whittaker, 1975). Progressive substitution by larger cations for tetrahedral silicon and by smaller cations for octahedral magnesium leads first to reduction of the misfit and then to larger dimensions of the tetrahedral sheet over the octahedral sheet. The effectiveness of such a mechanism for relief of misfit have been given by several authors. For instance, Roy and Roy (1954) took advantage of the larger ionic radius of germanium (0.40Å instead of 0.26Å of silicon, according to Shannon and Prewitt, 1969) and synthesized a $Mg_3Ge_2O_5(OH)_4$ serpentine that crystallized in euhedral hexagonal plates and produced sharp X-ray diffraction patterns. Many papers deal with the relationship between the Al_2O_3 content and the cylindrical or flat nature of the layers (*e.g.*, Roy and Roy, 1954; Nagy and Faust, 1956; Chernosky, 1975; Thomas *et al.*, 1979). Caruso and Chernosky (1979) described the increasing thermal stability of lizardite with the increasing Al_2O_3 content. Highly refined structure models resulting from a high degree of three-dimensional order have been produced only for aluminum-rich serpentine minerals (Jahanbagloo and Zoltai, 1968; Hall and Bailey, 1979; Anderson and Bailey, 1981; the present work). Therefore, it seems well established that the aluminum content (and, as a rule, any suitable substituent) is a very important factor in the crystal chemistry of the serpentine minerals.

In spite of the evidence for such a mechanism for relief of the misfit by fitting of dimensions, care is required with regard to the interpretation of these data. We must distinguish, for instance, between the mechanism accompanying the substitution of Ge^{4+} for silicon and that accompanying the substitution of Al^{3+} (or any other suitable trivalent cation).

In the first case, stabilization must be achieved by dimensional fitting of the two sheets. In the second case, the modified charge distribution inside the layer must also be taken into account. This was first noted by Gillery (1959), who stated that "the octahedral part acquires a positive charge and the tetrahedral a negative charge and the layer as a whole is neutral. The layer surfaces which face each other have opposite charge and this provides a force of attraction between them which increases with increasing aluminum content. Hence the basal spacing decreases with increasing aluminum content". Subsequently, Steadman and Nuttall (1963) invoked some kind of electrostatic interaction between the successive layers in the different polytypes of cronstedtite. The existence of electrostatic interaction between the 1:1 layers of kaolinite-like minerals was supported also by Cruz *et al.* (1972), who treated the minerals as condenser plates with surface charges due to hydroxyl dipoles. Giese (1973) showed that the electrostatic interaction in kaolinite-like minerals could be explained assuming that long hydrogen bonds are largely electrostatic in nature. Finally, Chernosky (1975) revived the hypothesis proposed by Gillery (1959) and once again related the reduction of the *c* parameter to the increasing charge difference between the two sheets. The hypothesis by Gillery did not seem to receive general acceptance. Several papers deal only with the geometrical fitting or misfitting between the two sheets of the layer, and do not take into account what happens between successive layers.

Other evidence seems to support the hypothesis of the existence of an "electrostatic" interaction which increases with an increasing substitution by trivalent cations. One argument is based on the basal spacing. The value increases from nearly 7.3Å in chrysotile polymorphs to 7.46Å in the Mg–Ge serpentine, in agreement with the larger ionic radius of germanium (0.40Å instead of 0.26Å for silicon, according to Shannon and Prewitt, 1969). On the other hand, the basal spacing is reduced to 7.08Å when aluminum (ionic radius 0.39Å) substitutes for silicon (*e.g.*, Chernosky, 1975) and to nearly 7.1Å when iron (0.49Å) substitutes for silicon (Steadman and Nuttall, 1963 and 1964). Although some account must be made for the smaller size of the octahedrally-coordinated aluminum and iron with respect to the octahedrally-coordinated magne-

sium, a definite decrease of the basal spacing is observed. This indicates that interlayer bonding is stronger than in Mg–Si or Mg–Ge serpentines.

A second indication that the interactions between adjacent layers in lizardite are stronger than in unsubstituted serpentine is given by their IR spectra. Farmer (1975) reports that the substitution of silicon by aluminum, compensated by replacement of magnesium by aluminum, gives two broad OH stretching absorption bands at lower frequencies than in chrysotile and antigorite. This indicates, according to Farmer (1975), a stronger hydrogen bond. A similar line of evidence is obtained from the IR data given by Heller-Kallai *et al.* (1975), who report similar IR absorption bands only for those specimens of serpentine which contain aluminum (according to them, these are five lizardites and two aluminous antigorites).

A further line of evidence can be found in the results of the present study. The average tetrahedral bond distance in lizardite 1*T* from Val Sissone, 1.639Å, does not differ too much from the expected value, 1.625Å, of a tetrahedron that contains only silicon (Shannon and Prewitt, 1969; the value is calculated taking into account the different coordination numbers of the oxygen atoms). The difference in bond distance does not seem large enough to support the idea that the high three-dimensional order of lizardite 1*T* may result from such slightly enlarged dimensions of the tetrahedral sheet.

Therefore, it seems reasonable to suppose that electrostatic interactions between adjacent layers, based on hydrogen bonds, exist and lead to stronger interlayer bonding. The mechanism can be formally described as substitution by trivalent cations for both tetrahedral silicon and octahedral magnesium, with a resultant excess of negative charge on the tetrahedral sheet and positive charge on the octahedral sheet. The negative charge is localized on the basal oxygen atoms of the tetrahedral sheet. The outer octahedral oxygens drain electrons from the more electropositive hydrogen atoms. These become positively charged, weakly acidic hydrogens. The separation of positive and negative charges on the two faces prevents curling of the layer and produces stronger interactions between adjacent layers, thus leading to flat structures.

An alternative formulation can be given if Pauling's rule is taken into account. The valences of the outer tetrahedral oxygens are undersaturated and the valences of the outer octahedral oxygens are oversaturated. Therefore octahedral oxygens weaken the bond they form with hydrogens. The bond valence balance is retained by formation of hydrogen bonds with undersaturated tetrahedral oxygen atoms. The structure, as a whole, has a lower energy, thus justifying the increasing thermal stability of substituted lizardite (Caruso and Chernosky, 1975).

Acknowledgments

Valuable criticism from the referees, Dr. M. Cameron and Dr. F. J. Wicks, is acknowledged. The specimen of lizardite and data about its occurrence were supplied by the collector Dr. E. Huen. Dr. P. Orlandi is gratefully acknowledged for providing the crystals of lizardite and the preliminary energy dispersive and scanning electron microscope results (obtained at the Istituto di Mineralogia dell' Università di Firenze). Many thanks are due to Prof. P.F. Zanazzi, Istituto di Mineralogia dell' Università di Perugia, for collecting X-ray diffraction intensity data. Last but not least, I thank the colleagues of the Istituto di Mineralogia dell' Università di Modena, who made available to me their electron microprobe laboratory.

References

Anderson, C. S. and Bailey, S. W. (1981) A new cation ordering pattern in amesite-$2H_{-2}$. American Mineralogist, 66, 185–195.

Bailey, S. W. (1969) Polytypism of trioctahedral 1 : 1 layer silicates. Clays and Clay Minerals, 17, 355–371.

Bailey, S. W. (1975) Cation ordering and pseudosymmetry in layer silicates. American Mineralogist, 60, 175–187.

Baronnet, A. (1976) Polytipisme et polymorphisme dans les micas. Contribution a l'etude du role de la croissance cristalline. Thesis, Universitè d' Aix Marseille III.

Baur, W. H. (1978) Variation of mean Si–O bond lengths in silicon-oxygen tetrahedra. Acta Crystallographica, B34, 1751–1756.

Brown, I. D. and Wu, K. K. (1976) Empirical parameters for calculating cation–oxygen bond valences. Acta Crystallographica, B32, 1957–1959.

Caruso, L. J. and Chernosky, J. V. (1979) The stability of lizardite. Canadian Mineralogist, 17, 757–769.

Chernosky, J. V. (1975) Aggregate refractive indices and unit cell parameters of synthetic serpentine in the system $MgO–Al_2O_3–SiO_2–H_2O$. American Mineralogist, 60, 200–208.

Cruz, M., Jacobs, J., and Fripiat, J. J. (1972) The nature of the cohesion energy in kaolin minerals. International Clay Conference, Madrid, 35–43.

Dungan, M. A. (1979) A microprobe study of antigorite and some serpentine pseudomorphs. Canadian Mineralogist, 17, 771–784.

Farmer, V. C. (1975) The infrared spectra of minerals. Mineralogical Society Monograph, 4, London.

Frost, B. R. (1975) Contact metamorphism of serpentinite, chloritic blackwall and rodingite at Paddy-Go-Easy Pass, Central Cascades, Washington. Journal of Petrology, 16, 272–313.

Franzini, M. (1969) The *A* and *B* mica layers and the crystal structure of sheet silicates. Contributions to Mineralogy and Petrology, 21, 203–224.

Giese, R. F. (1973) Interlayer bonding in kaolinite, dickite and nacrite. Clays and Clay Minerals, 21, 145–149.

Gillery, F. H. (1959) The X-ray study of synthetic Mg-Al serpentines and chlorites. American Mineralogist, 44, 143–152.

Hall, S. H. (1974) The triclinic structure of amesite. M.S. Thesis, University of Wisconsin, Madison.

Hall, S. H. and Bailey, S. W. (1979) Cation ordering pattern in amesite. Clays and Clay Minerals, 27, 241–247.

Hall, S. H., Guggenheim, S., Moore, P., and Bailey, S. W. (1976) The structure of Unst-type 6-layer serpentines. Canadian Mineralogist, 14, 314–321.

Heller-Kallai, L., Yariv, Sh., and Gross, S. (1975) Hydroxyl stretching frequencies of serpentine minerals. Mineralogical Magazine, 40, 197–200.

International Tables for X-ray Crystallography, vol. IV (1974). Kynoch Press, Birmingham.

Jahanbagloo, J. C. and Zoltai, T. (1968) The crystal structure of a hexagonal Al-serpentine. American Mineralogist, 53, 14–24.

Jasmund, K. and Sylla, H. M. (1971) Synthesis of Mg- and Ni-antigorite. Contributions to Mineralogy and Petrology, 34, 84–86.

Jasmund, K. and Sylla, H. M. (1972) Synthesis of Mg- and Ni-antigorite: a correction. Contributions to Mineralogy and Petrology, 34, 346.

Krstanovic, I. (1968) Crystal structure of single-layer lizardite. Zeitschrift für Kristallographie, 126, 163–169.

Krstanovic, I. (1980) Crystal structure of flat-layer serpentine minerals. Abstracts of the 26th International Geological Congress, Paris.

Lippincott, E. R. and Schroder, R. (1955) One dimensional model of the hydrogen bond. Journal of Chemical Physics, 23, 1099–1106.

Nagy, B. and Faust, G. T. (1956) Serpentine: natural mixtures of chrysotile and antigorite. American Mineralogist, 39, 957–975.

O'Keeffe, M. and Hyde, B. G. (1978) On Si–O–Si configuration in silicates. Acta Crystallographica, B34, 27–32.

Peterson, R. C., Hill, R. J., and Gibbs, G. V. (1979) A molecular-orbital study of distortions in the layer structures brucite, gibbsite and serpentine. Canadian Mineralogist, 17, 703–711.

Radoslovich, E. W. (1962) The cell dimensions and symmetry of layer lattice silicates. II. Regression relations. American Mineralogist, 47, 617–636.

Rayner, J. H. and Brown, G. (1973) The crystal structure of talc. Clays and Clay Minerals, 21, 103–114.

Roy, D. M. and Roy, R. (1954) An experimental study of the formation and properties of synthetic serpentines and related layer silicate minerals. American Mineralogist, 39, 957–975.

Rozenson, I., Banninger, E. R., and Heller-Kallai, L. (1979) Mössbauer spectra of iron in 1 : 1 phyllosilicates. American Mineralogist, 64, 893–901.

Rucklidge, J. C. and Zussmann, J. (1965) The crystal structure of the serpentine mineral, lizardite $Mg_3Si_2O_5(OH)_4$. Acta Crystallographica, 19, 381–389.

Shannon, R. D. and Prewitt, C. T. (1969) Effective ionic radii in oxides and fluorides. Acta Crystallographica, B25, 925–946.

Shirozu, H. and Bailey, S. W. (1965) Chlorite polytypism: III. Crystal structure of an orthohexagonal iron chlorite. American Mineralogist, 50, 868–885.

Steadman, R. and Nuttall, P. M. (1962) The crystal structure of amesite. Acta Crystallographica, 15, 510–511.

Steadman, R. and Nuttall, P. M. (1963) Polymorphism in cronstedtite. Acta Crystallographica, 16, 1–8.

Steadman, R. and Nuttall, P. M. (1964) Further polymorphism in cronstedtite. Acta Crystallographica, 17, 404–406.

Steinfink, H. and Brunton, G. (1956) The crystal structure of amesite. Acta Crystallographica, 9, 487–492.

Thomas, J. M., Jefferson, D. A., Mallinson, L. G., Smith, D. G., and Crawford, E. S. (1979) The elucidation of the ultrastructure of silicate minerals by HREM and X-ray emission microanalysis. In L. Kihlborg, Ed., Direct Imaging of Atoms and Molecules in Crystals. The Royal Swedish Academy of Sciences, Stockolm.

Trommsdorf, V. and Evans, B. W. (1972) Progressive metamorphism of antigorite schist in the Bergell tonalite aureole (Italy). American Journal of Science, 272, 423–437.

Trommsdorf, V. and Evans, B. W. (1977) Antigorite ophicarbonates: contact metamorphism in Valmalenco, Italy. Contributions to Mineralogy and Petrology, 62, 423–437.

Wenk, H. R. and Maurizio, R. (1970) Geological observations in the Bergell area (SE-Alps). II. Contact minerals from Mt. Sissone-Cima di Vazzeda (A mineralogical note). Schweitzerische Mineralogische und Petrographische Mitteilungen, 50, 349–354.

Whittaker, E. J. W. and Wicks, F. J. (1970) Chemical differences among the serpentine "polymorphs": a discussion. American Mineralogist, 55, 1025–1047.

Whittaker, E. J. W. and Zussmann, J. (1956) The characterization of serpentine minerals by X-ray diffraction. Mineralogical Magazine, 31, 107–126.

Wicks, F. J. and Plant, A. G. (1979) Electron-microprobe and X-ray-microbeam studies of serpentine textures. Canadian Mineralogist, 17, 785–830.

Wicks, F. J. and Whittaker, E. J. W. (1975) A reappraisal of the structures of the serpentine minerals. Canadian Mineralogist, 13, 227–243.

Manuscript received, May 22, 1981;
accepted for publication, December 30, 1981.